

The spectral line Ba II 6497 Å as a sensitive Doppler diagnostics

J. Koza

*Astronomical Institute of the Slovak Academy of Sciences
059 60 Tatranská Lomnica, The Slovak Republic, (E-mail: koza@astro.sk)*

Received: February 24, 2011; Accepted: April 13, 2011

Abstract. We present a quantitative and comparative analysis of sensitivity to the line-of-sight velocity of the spectral line Ba II 6497 Å identified as a very promising Doppler mapper of the solar photosphere and low chromosphere. We examine its sensitivity to changes of the line-of-sight velocity by sharpness of its line profile and the response function to the line-of-sight velocity evaluated by the 1-D model of the quiet solar atmosphere in the LTE approximation. We compare its sensitivity with selected barium, iron, and chromium lines widely used in the diagnostics of the solar photosphere. The set of selected lines includes the Ba II 4554 Å line, generally considered to be an excellent Doppler mapper. The comparison clearly shows that the line Ba II 6497 Å is one of the most sensitive from the lines included in our set. This is due to a favorable combination of a relatively sharp line profile and a long wavelength implying a large Doppler sensitivity. The line Ba II 6497 Å offers many advantages, making it a highly recommendable choice for dedicated studies of line-of-sight velocities in the photosphere and low chromosphere.

Key words: Sun: photosphere – Line: formation – Line: profiles

1. Introduction

Photospheric line-of-sight velocities (henceforth velocities) are traditionally studied by means of a small set of metallic lines selected considering their effective Landé factor, atomic weight, steepness of flanks, and wavelength. A larger atomic weight means a smaller thermal broadening of a spectral line profile, implying its reduced sensitivity to thermal inhomogeneities in favor of larger sensitivity to non-thermal motions. This fact and a rectangular shape with steep flanks made the resonance line of Ba II 4554 Å renowned as an excellent Doppler diagnostic of photospheric velocities using the tunable Lyot filter built at the Irkutsk Institute of Solar-Terrestrial Physics (Kushtal, Skomorovsky 2002) and installed at the Dutch Open Telescope as part of its multi-wavelength speckle imaging system (Rutten *et al.*, 2004).

A recent advance has been the identification of the simple rules enabling us to characterize the sensitivity of weak photospheric lines to velocity by means of their response functions in the study of Cabrera Solana *et al.* (2005). These

authors introduce an exact quantitative definition of the sensitivity of a spectral line to a particular atmospheric parameter allowing them to compare the sensitivity of spectral lines and to identify the most sensitive ones for a given atmospheric model. Their method based on response functions shows that the sensitivity of a spectral line to velocity is given not only by its wavelength but primarily by its sharpness defined as the ratio between the depth and the width of a line.

The method of Cabrera Solana *et al.* (2005) has been applied extensively in Koza (2010) (henceforth Paper I) with the aims to examine and compare the sensitivity of selected barium, iron, and chromium spectral lines to velocity changes and to demonstrate the applicability of the method for different spectral lines and a different atmospheric model than those used in the original work of Cabrera Solana *et al.* (2005). The set of selected lines included the barium lines Ba II 4554 Å and 6497 Å. The latter was already used in the studies of granular velocities (Mattig, Schlebbe 1974; Mattig, Nesis 1976; Durrant *et al.*, 1979), velocity oscillations in sunspot umbrae (Soltau *et al.*, 1976), depth dependence of photospheric oscillations (Koch *et al.*, 1979), and in high-resolution spectroscopy of the solar photosphere (Wiehr, Kneer 1988; Hanslmeier *et al.*, 1991).

This paper supplements Paper I with the aim of highlighting more a large Doppler sensitivity of the Ba II 6497 Å line and its diagnostic properties, making it a highly recommendable choice for dedicated studies of velocities in the photosphere and low chromosphere. We extend the results given in Paper I showing explicitly the derivatives of the atlas and synthetic profiles of Ba II 6497 Å and its depth-integrated response function to velocity. Since we will refer to Paper I very often, we invite the reader to have it handy.

2. Calculations and results

As Cabrera Solana *et al.* (2005) suggest, the sensitivity of a spectral line to velocity can be estimated by means of its profile extracted from a spectral atlas or the synthetic profile or the response function. In our paper we employ all these approaches using the solar spectral atlas (Neckel, 1999) as the source of the disk center profile of Ba II 6497 Å. Its synthetic profile and response function to velocity (RF_V henceforth) are computed simultaneously in LTE using the SIR code (Ruiz Cobo, del Toro Iniesta 1992), the atmospheric model of Holweger and Müller (1974), and the atomic parameters in Tab. 1 of Paper I, but using the standard formula for the collisional broadening (Unsöld, 1968) with the enhancement factor set to 0.7 instead of the parameters α and σ found in Paper I as inadequate. The extensive hyperfine and isotopic structure of Ba II 6497 Å is simplified by four components as suggested by Rutten (1976, 1978). Central wavelengths and oscillator strengths of the four components in Tab. 1 of Paper I are computed from the data given in Rutten (1976, 1978). Since the method of Cabrera Solana *et al.* (2005) operates with the depth-integrated response

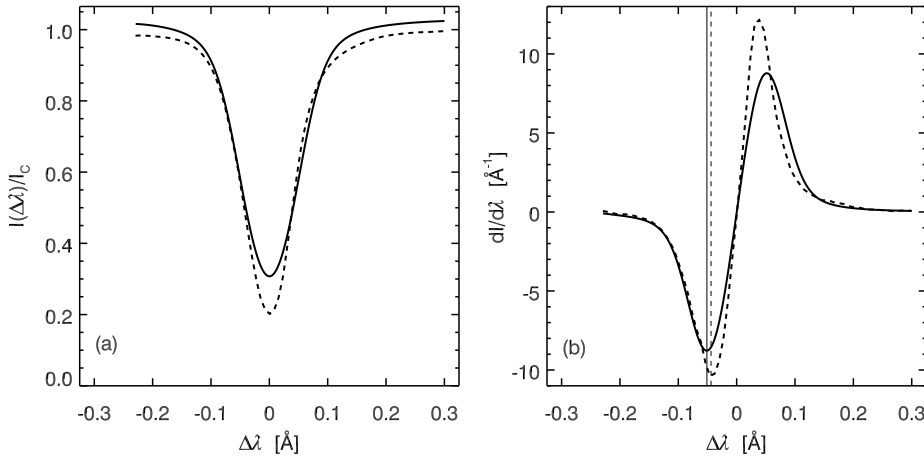


Figure 1. Atlas (dashed) and synthetic (solid) disk center profiles of the spectral line Ba II 6497 Å (a) computed by the solar atmospheric model of Holweger and Müller (1974). Derivatives $dI/d\lambda$ of the atlas (dashed) and synthetic (solid) disk center profile (b). The thin vertical dashed and solid line indicates the wavelength of minimum of the derivative of the atlas and synthetic profile, respectively.

function to velocity (IRF_V henceforth) assuming a constant perturbation of velocity with height h , we perform an integration of $RF_V(\Delta\lambda, h)$ along its spatial scale to obtain relevant IRF_V($\Delta\lambda$).

Fig. 1a shows the atlas and synthetic disk center profile of Ba II 6497 Å computed by the model of Holweger and Müller (1974). The good agreement of the flanks of the synthetic and atlas profile indicates the adequacy of the adopted model of Holweger and Müller (1974), the four-component simplification of the hyperfine and isotopic structure, and LTE everywhere except the line core, which disagrees similarly as in Holweger and Müller (1974). This disagreement influences estimates of the sensitivity of Ba II 6497 Å to velocity based on the shape ratios (Paper I) of the atlas and synthetic profile and its IRF_V (Fig. 2).

Fig. 1b shows derivatives of the atlas and synthetic profile as a quantitative characteristic of the steepness of Ba II 6497 Å line flanks. This is one of the indicators of usefulness of the line in velocity measurements by narrowband filters since the same velocity induces a larger Doppler signal for a line with steeper flanks and a longer wavelength. The minimum (maximum) of the derivative of the synthetic and atlas profile occurs at $\Delta\lambda = -51$ (52) and -44 (39) mÅ, respectively. These suggest the optimum wavelength settings of narrowband filters promising to bring the largest Doppler signal even for small velocities.

Fig. 2a shows RF_V of Ba II 6497 Å multiplied by the spatial step of the atmospheric model $\Delta \log \tau_{5000} = 0.1$. Its shape clearly demonstrates that the maximum of sensitivity to velocity changes does not occur at the line center but in the wings. In addition, velocity changes in the low photosphere at a height of

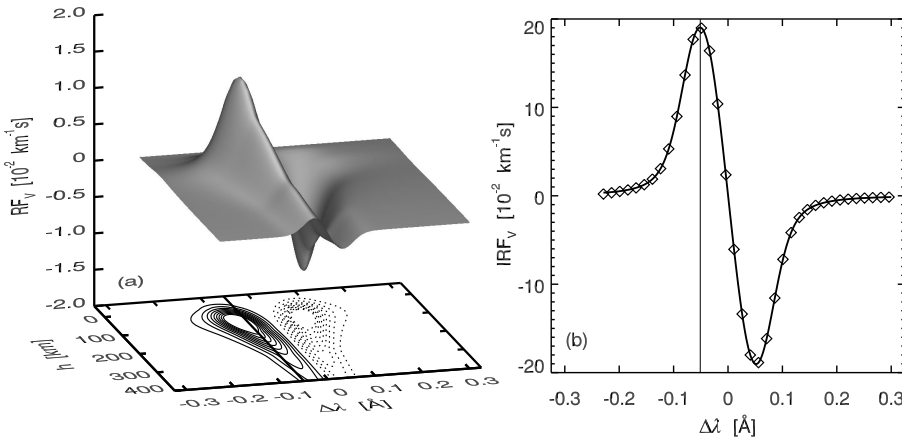


Figure 2. A response function to velocity RF_V of the spectral line Ba II 6497 Å (a) normalized to the HSRA continuum at the disk center at the central wavelength of the line. The $(\Delta\lambda, h)$ plane: the solid line indicates the wavelength of maximum λ_{\max} of the depth-integrated response function IRF_V ; solid and dashed contours distinguish positive and negative lobe of RF_V , respectively. IRF_V (solid) of the spectral line Ba II 6497 Å (b). The thin solid vertical line indicates the wavelength of its maximum λ_{\max} shown also in the panel (a) in the $(\Delta\lambda, h)$ plane. The diamonds represent the values computed by equation (2).

~ 100 km induce the largest intensity variations in the wings. Positive and negative lobes mean that a small positive velocity change increases intensity in the blue wing and decreases it in the red wing, making the spectral line asymmetric. But both the synthetic profile and RF_V (Figs. 1a and 2a) are intrinsically asymmetric even in the case of zero velocity in the applied model of Holweger and Müller (1974) due to the hyperfine and isotopic structure of Ba II 6497 Å.

Fig. 2b shows IRF_V of Ba II 6497 Å, which is more suitable than RF_V for a quantitative analysis of sensitivity comparing different lines. Like RF_V , IRF_V plays the role of the partial derivative $\partial I / \partial v$ of the emergent intensity with respect to the velocity but assuming its height independent perturbation (Cabrera Solana *et al.*, 2005). The maximum and minimum of IRF_V occur at $\Delta\lambda = -51$ mÅ and 52 mÅ. Interestingly, these equal to the wavelengths of extremes of the derivative of the synthetic Ba II 6497 Å profile in Fig. 1b.

3. Comparisons

We used the atlas and synthetic profiles of the selected spectral lines (see Tab. 1 in Paper I) to determine their depths A_0 , widths A_1 , shape ratios A_0/A_1 , and maxima of IRF_V referred to in the following as $IRF_V(\lambda_{\max})$ and computed as

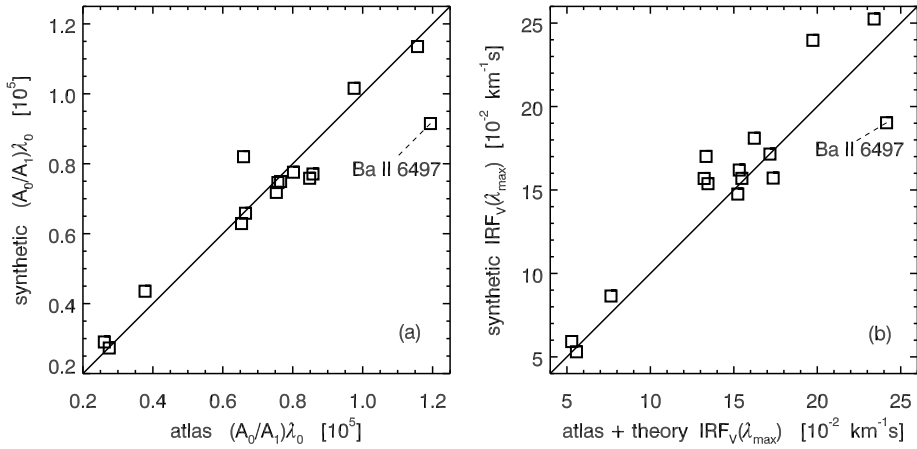


Figure 3. Shape ratios A_0/A_1 of the selected spectral lines (see Paper I) measured on their atlas and synthetic profiles multiplied by the central wavelength λ_0 (a). Maxima of the depth-integrated response functions $IRF_V(\lambda_{\max})$ (y axis) *versus* the values computed by equation (1) (x axis) using the shape ratios of the atlas profiles multiplied by the central wavelengths λ_0 of the spectral lines (b). Thick lines indicate diagonals.

$$IRF_V(\lambda_{\max}) = e^{-1/2} \frac{A_0}{A_1} \frac{\lambda_0}{c}. \quad (1)$$

The widths A_1 are in fact Doppler half-widths computed from measured FWHM of the atlas and synthetic profiles as $A_1 = \text{FWHM}/(2\sqrt{\ln 2})$. The theoretical background of equation (1) and explanation of individual symbols are given in Cabrera Solana *et al.* (2005) and in Paper I as well. Further, we employed the computed IRF_V (*e.g.*, Fig. 2b) to determine their maxima $IRF_V(\lambda_{\max})$ referred to in the following plots as the synthetic $IRF_V(\lambda_{\max})$ to distinguish them from $IRF_V(\lambda_{\max})$ computed by equation (1).

Fig. 3a shows the shape ratios A_0/A_1 of the atlas and synthetic profiles multiplied by their central wavelengths λ_0 . The plot enables us to compare the sensitivity of the spectral lines to velocity changes through equation (1), since the larger the product $(A_0/A_1)\lambda_0$, the larger the sensitivity. The deviations from the diagonal indicate disagreements of the synthetic and atlas profiles and thus the relevance of the information derived afterwards from IRF_V . The largest deviation shows the synthetic profile of Ba II 6497 Å, whose line core is much shallower than the core of its atlas profile (Fig. 1a). Fig. 3a suggests that Ba II 6497 Å has a similar sensitivity to Fe I 5247 Å identified in Cabrera Solana *et al.* (2005) as the most sensitive spectral line to velocity changes in the quiet solar photosphere. Although the Ba II 6497 Å line profile is broader than that of Fe I 5247 Å (see Paper I), its longer wavelength causes a larger Dopplershift and thus large sensitivity to velocity.

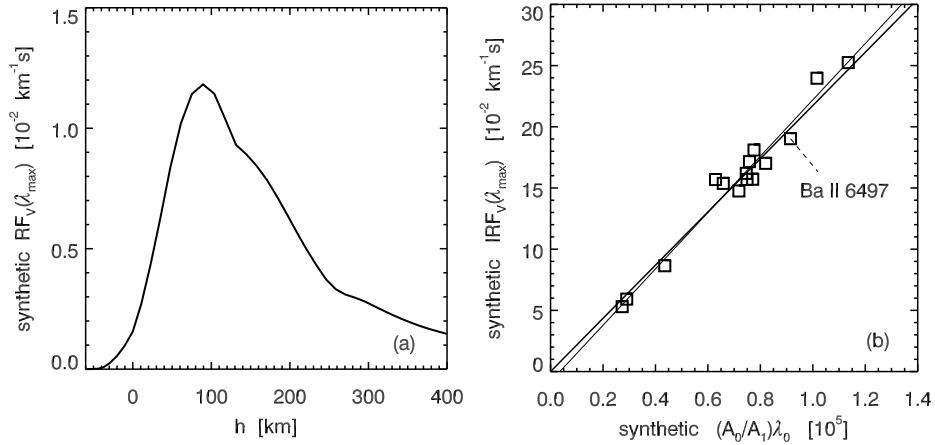


Figure 4. Cross-section of the response function to velocity RF_V of Ba II 6497 Å shown in Fig. 2a at the wavelength of maximum λ_{\max} of its depth-integrated response function IRF_V (a). Maxima of the depth-integrated response functions $IRF_V(\lambda_{\max})$ (y axis) *versus* the shape ratios of the synthetic profiles multiplied by the central wavelengths λ_0 of the selected spectral lines (b). The thick line indicates a linear fit of the data in Fig. 2 by Cabrera Solana *et al.* (2005). The thin line is a linear fit of our data.

Fig. 3b shows the synthetic $IRF_V(\lambda_{\max})$ *versus* $IRF_V(\lambda_{\max})$ computed by equation (1) using the shape ratios A_0/A_1 of the atlas profiles. Since the data approximately follow the diagonal, we consider this plot as a proof of the adequacy of the adopted assumptions and the method of Cabrera Solana *et al.* (2005). The plot indicates again the large sensitivity to velocity of Ba II 6497 Å. A large deviation of the Ba II 6497 Å datapoint from the diagonal is caused by a large discrepancy of its atlas and synthetic line core seen in Fig. 1a.

Fig. 4a shows the cross-section of RF_V (Fig. 2a) made at the wavelength of maximum λ_{\max} of IRF_V (Fig. 2b). The plot demonstrates that the sensitivity of Ba II 6497 Å is significant within the height interval ranging from 50 to 200 km assuming the model of Holweger and Müller (1974) with zero velocity. Following Cabrera Solana *et al.* (2005) we show in Fig. 4b the synthetic $IRF_V(\lambda_{\max})$ as a function of the product of shape ratios with the central wavelengths $(A_0/A_1)\lambda_0$ for the synthetic line profiles. A linear trend followed from our data implies that equation (1) correctly describes the relation between the sensitivity of spectral lines to velocity and their parameters. The close similarity of the two linear fits shown in Fig. 4b verifies our results with respect to the results of Cabrera Solana *et al.* (2005). As this plot shows, the lines Fe I 5247 Å, Cr I 5248 Å, and Ba II 6497 Å are most sensitive to velocity changes from the lines in Tab. 1 of Paper I. However, a better modeling of Ba II 6497 Å would show that this line is the most sensitive one of the selected spectral lines. This is indicated by the quantities derived from its atlas profile and shown in Figs. 3a and 3b.

4. Discussion

We obtained the results presented in the previous section assuming a stationary atmosphere with zero velocity. But the atmosphere of the real Sun involves non-zero velocities with vertical gradients. The question is how this influences RF_V of a particular line. Koza and Kučera (2003) show that the presence of non-zero velocity with a height gradient in an atmospheric model causes a strong velocity-induced asymmetry of RF_V . In a particular case of the granular model applied in Koza and Kučera (2003) one lobe of RF_V is shifted towards upper photospheric layers while the other occupies the lower photosphere. Then the question is whether the strong asymmetry of RF_V would influence the relevant values of synthetic $IRF_V(\lambda_{max})$ used in the comparison of sensitivity of individual lines (Figs. 3b and 4b). To find the answer, an analysis similar to that in Paper I is needed, but involving a more realistic model of the solar atmosphere.

Durrant *et al.* (1979) show a line center velocity weighting function of Ba II 6497Å. Although this historical name introduced by Mein (1971) implies its correspondence with RF_V , the velocity weighting function $W_v(h)$ shown there is not a genuine RF_V representing intensity variations. In fact, it is a line shift response function introduced originally in Canfield (1976) as a specific *ad-hoc* construct of response function to velocity with its depth-integrated version $C(\Delta\lambda)$.

At the end of section 2 we have pointed out an interesting equality of wavelengths of IRF_V extremes (Fig. 2b) and the derivative $\partial I / \partial \lambda$ (Fig. 1b). As we will show, this is a direct consequence of a link between $d\partial I / \partial \lambda$ and IRF_V representing the derivative $\partial I / \partial v$. Combining the Doppler relation $\partial v = (-c/\lambda)\partial\lambda$ with $\partial I / \partial v$ one can easily show that

$$\frac{\partial I}{\partial v} = -\frac{\lambda}{c} \frac{\partial I}{\partial \lambda}. \quad (2)$$

This equation can be found in Canfield (1976). For a particular case of the line Ba II 6497Å, equation (2) can be rewritten as $\partial I / \partial v = -2.17 \partial I / \partial \lambda$ with the appropriate unit $10^{-2} \text{ km}^{-1}\text{s}$. The values of $\partial I / \partial v$ calculated by the latter equation are shown in Fig. 2b by diamonds. The close correspondence of both types of values in Fig. 2b suggests a practical application of equation (2). One can calculate IRF_V of any spectral line straightforwardly by equation (2) and the derivative of either its atlas or synthetic profile. Equation (2) clearly shows that the intensity variation induced by a velocity change $\partial I / \partial v$ is determined by both the steepness of the line profile $\partial I / \partial \lambda$ and its wavelength λ . Since this relation is general, it can be used in examination of the sensitivity to velocity of strong chromospheric lines beyond the limit of a weak line model assumed in Cabrera Solana *et al.* (2005).

5. Summary

We have applied the method of Cabrera Solana *et al.* (2005) to examine the sensitivity of selected spectral lines to velocity changes by the sharpness of their line profiles and the response functions to velocity evaluated by the quiet Sun model of Holweger and Müller (1974) in the LTE approximation. Our results demonstrate the applicability of the method for different spectral lines and a different atmospheric model than those used in the original work of Cabrera Solana *et al.* (2005). This proves the adequacy of the weak line model and the assumptions which the method is based on. We recognize a new Doppler mapper of the solar photosphere and low chromosphere, which is the line Ba II 6497 Å. It combines the advantages of a large sensitivity to velocity with a small thermal broadening due to a large atomic weight and a generally favorable response of detectors within its spectral domain. Moreover, its line center maps velocities in the low chromosphere. All this makes Ba II 6497 Å a highly recommendable choice for dedicated studies of line-of-sight velocities in the photosphere and low chromosphere.

Acknowledgements. This work was supported by the VEGA grant 2/0064/09.

References

- Cabrera Solana, D., Bellot Rubio, L.R., del Toro Iniesta, J.C.: 2005, *Astron. Astrophys.* **439**, 687
 Canfield, R.C.: 1976, *Sol. Phys.* **50**, 239
 Durrant, C.J., Mattig, W., Nesis, A., Reiss, G., Schmidt, W.: 1979, *Sol. Phys.* **61**, 251
 Hanslmeier, A., Mattig, W., Nesis, A.: 1991, *Astron. Astrophys.* **244**, 521
 Holweger, H., Müller, E.A.: 1974, *Sol. Phys.* **39**, 19
 Koch, A., Käveler, G., Schröter, E.H.: 1979, *Sol. Phys.* **64**, 13
 Koza, J.: 2010, *Sol. Phys.* **266**, 261 (Paper I)
 Koza, J., Kučera, A.: 2003, *Contrib. Astron. Obs. Skalnaté Pleso* **33**, 224
 Kushtal, G.I., Skomorovsky, V.I.: 2002, in *Proc. SPIE*, eds.: Y.V. Chugui, S.N. Bagayev, A. Weckenmann, and P.H. Osanna, 4900, 504,
 Mattig, W., Nesis, A.: 1976, *Sol. Phys.* **50**, 255
 Mattig, W., Schlebbe, H.: 1974, *Sol. Phys.* **34**, 299
 Mein, P.: 1971, *Sol. Phys.* **20**, 3
 Neckel, H.: 1999, *Sol. Phys.* **184**, 421
 Ruiz Cobo, B., del Toro Iniesta, J.C.: 1992, *Astrophys. J.* **398**, 375
 Rutten, R.J.: 1976, *Solar Eclipse Observations and Ba II Line Formation*, PhD Thesis, University of Utrecht
 Rutten, R.J.: 1978, *Sol. Phys.* **56**, 237
 Rutten, R.J., Hammerschlag, R.H., Bettonvil, F.C.M., Sütterlin, P., de Wijn, A.G.: 2004, *Astron. Astrophys.* **413**, 1183
 Soltau, D., Schröter, E.H., Wöhl, H.: 1976, *Astron. Astrophys.* **50**, 367
 Unsöld, A.: 1968, *Physik der Sternatmosphären mit besonderer Berücksichtigung der Sonne*, Berichtiger Nachdruck der zweiten Auflage, Springer-Verlag, Berlin
 Wiehr, E., Kneer, F.: 1988, *Astron. Astrophys.* **195**, 310